Electronic Supplementary Material (ESI) for Nanoscale
This journal is © Royal Society of Chemistry 2014

Supplementary Information

Desired crystal orientated $LiFePO_4$ nanoplatelets *in situ* anchored on a graphene cross-linked conductive network for fast lithium storage

Bo Wang,[ab] Anmin Liu,[a] Wael Al Abdulla,[c] Dianlong Wang*[a] and X. S. Zhao*[bd]

[a] Harbin Institute of Technology, School of Chemical Engineering and Technology, Xidazhi Street, 150001 Harbin, China. Fax: 86 451 86413721; Tel: 86 451 86413751; E-mail: wangdianlongwbhit@163.com

[b] The University of Queensland, School of Chemical Engineering, St Lucia, Brisbane, QLD 4072, Australia. Fax: 61 7 33654199; Tex: 61 7 33469997; E-mail: george.zhao@uq.edu.au

[c] The University of Queensland, Australian Institute for Bioengineering and Nanotechnology, St. Lucia, Brisbane, QLD 4072, Australia.

[d] Qingdao University, Colloge of Chemical Science and Engineering, Qingdao 207661, China.

Statistical calculation of the proportion for (010) facet

Based on the observation from both SEM and TEM mesurement, a cuboid modle was adopted to calculate the proportion of (010) facet, as shown in Scheme S1†.

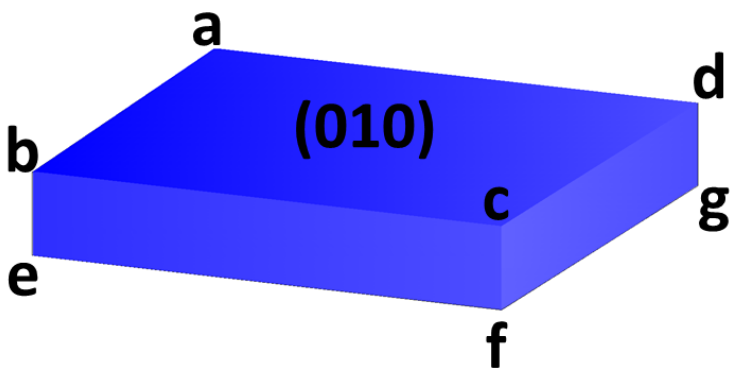

Scheme S1† Schematic model of an ideal LFP platelet with the largest (010) exposed facet.

From Scheme S1†, we can calculated the surface area (*S*) of each plane by the following equations:

$$S(010) = S(abcd) = ab \times bc;$$

$$S(bcfe) = bc \times be;$$

$$S(cdgf) = cd \times cf;$$

Therefore, the proportion of (010) facet can be obtained by dividing the surface area of (010) facet by the total surfaces area using the following equation:

$$\mathrm{S(010)\%} = \frac{S(abcd)}{S(abcd)+S(bcfe)+S(cdgf)} \times 100\,\% = \frac{\mathrm{ab}\times\mathrm{bc}}{\mathrm{ab}\times\mathrm{bc}+\mathrm{bc}\times\mathrm{be}+\mathrm{cd}\times\mathrm{cf}} \times 100\,\%$$

The lengths of *ab* (*cd*), *bc* and *be* (*cf*) have been estimated by gathering statistics of dozens of relatively regular platelets, and then calculated the average values. Due to the same LFP component of LFP and LFP/GNs, here, we only chose LFP as the representative. The final values of the statistical length and the calculated proportion of (010) facet were listed in Table S3† for comparison.

Figures

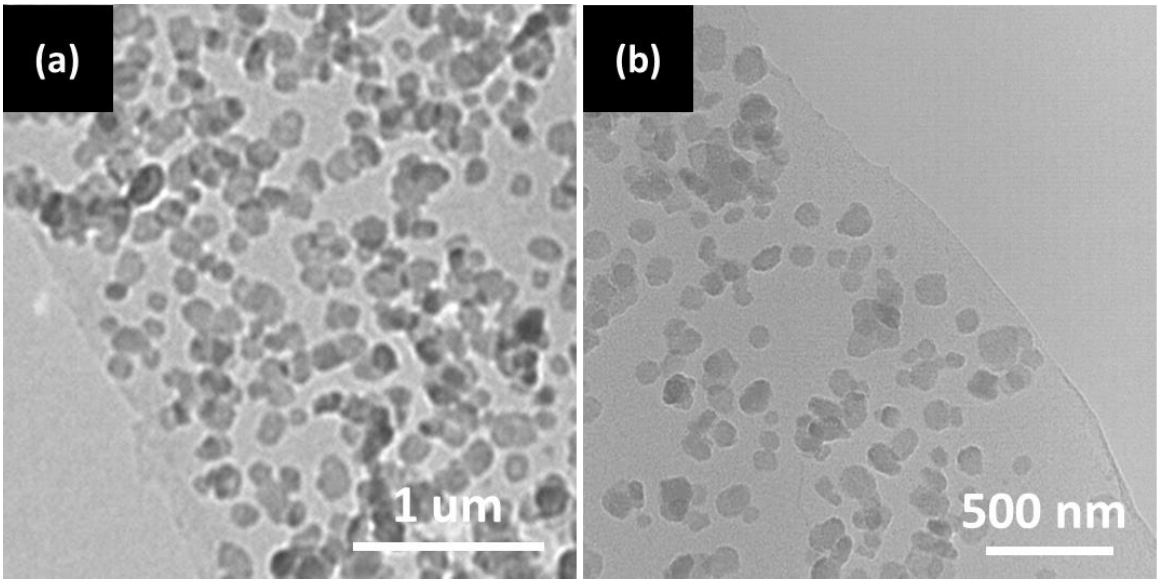

Fig. S1† TEM images of LFP@GNs.

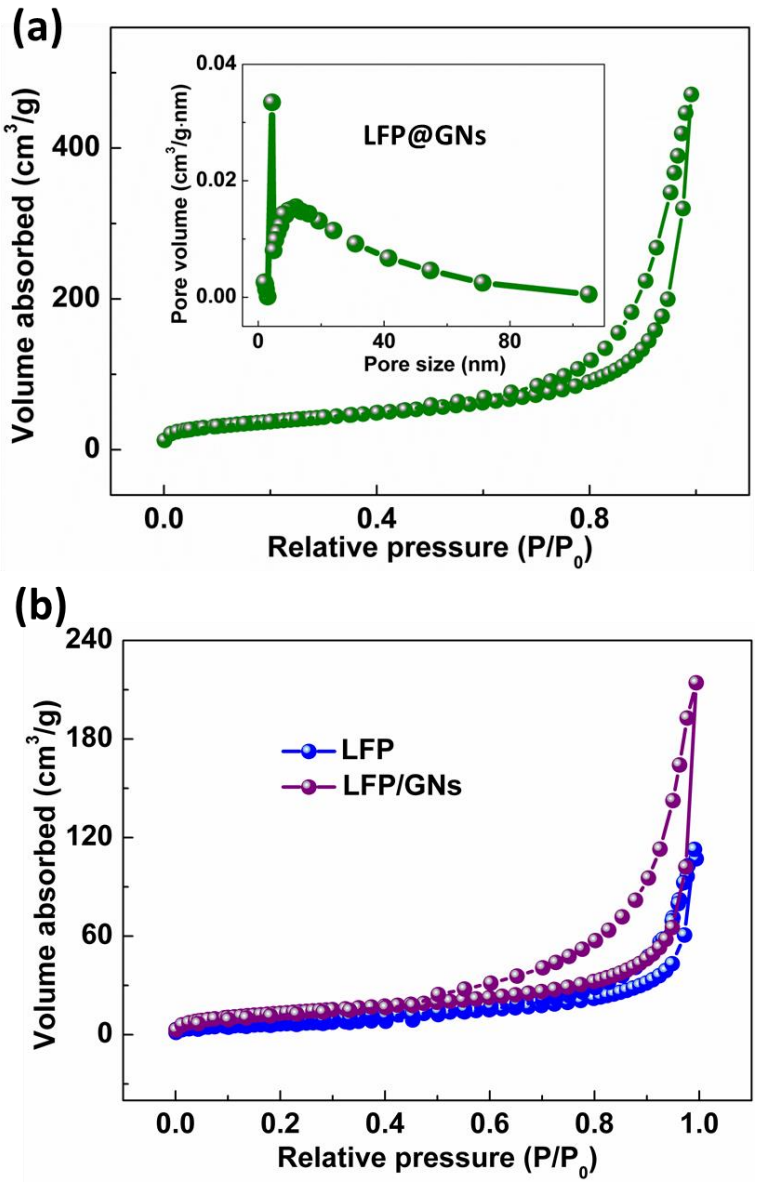

Fig. S2† (a) Nitrogen adsorption/desorption isotherms and pore-size distribution curves of LFP@GNs and (b) Nitrogen adsorption/desorption isotherms of LFP and LFP/GNs.

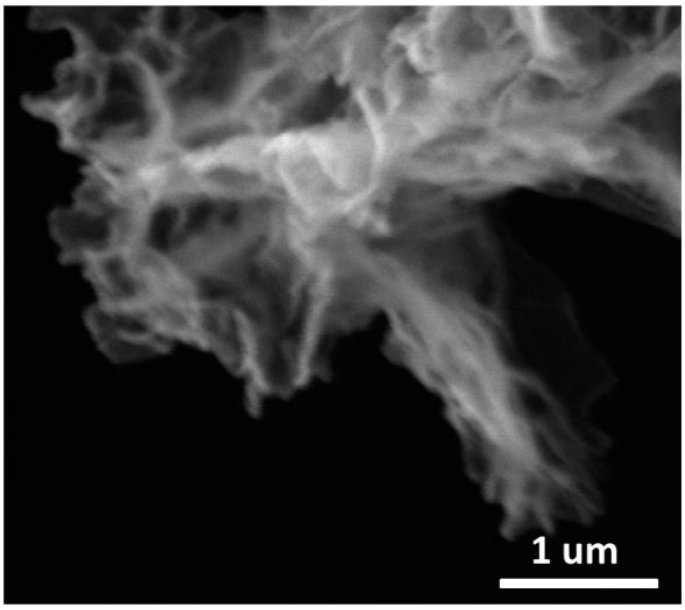

Fig. S3† SEM image of a 3D graphene cross-linked conductive network obtained by removing LFP platelets with an HCl solution.

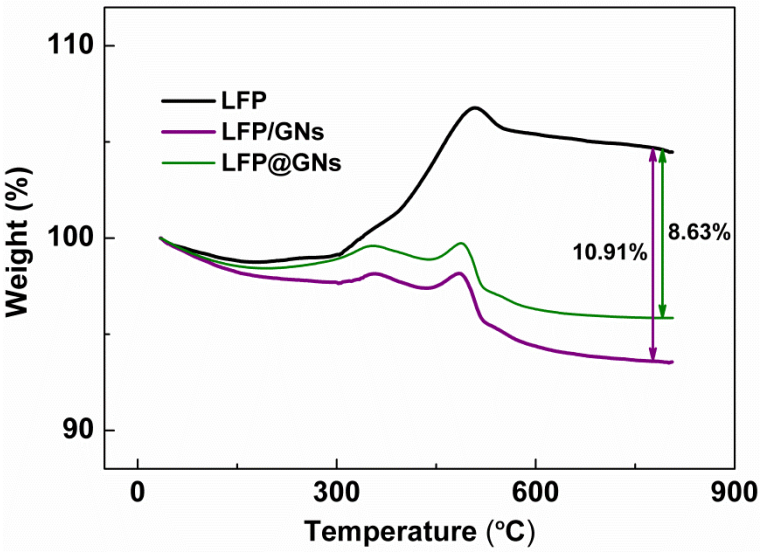

Fig. S4† TGA curves of LFP, LFP/GNs and LFP@GNs.

The graphene contents of LFP/GNs and LFP@GNs were revealed by thermogravimetric analysis (TGA). In the thermogravimetric curves, the weight changed over three steps appearing at 100-320 ℃, 320-430 ℃ and 430-630 ℃. For the first step, the weight loss was mainly due to the water evaporation. At the second step, LFP gained weight due to Fe^{2+} oxidation in air. The carbon oxidation occurred over all the three steps, and consequently, the weight was reduced. Thereby, the weight loss from carbon decomposition can represent the carbon content in the samples. Yielded graphene contents of LFP/GNs and LFP@GNs were 10.91 and 8.63 wt.%, respectively.[1,2]

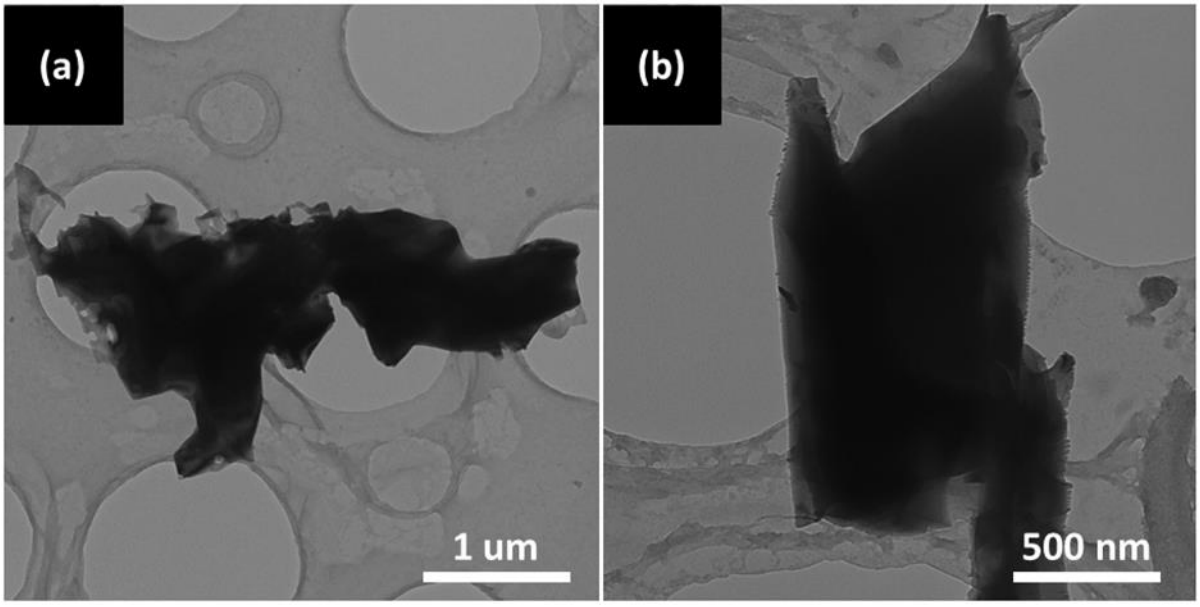

Fig. S5† TEM images of LFP synthesized using water as the single solvent.

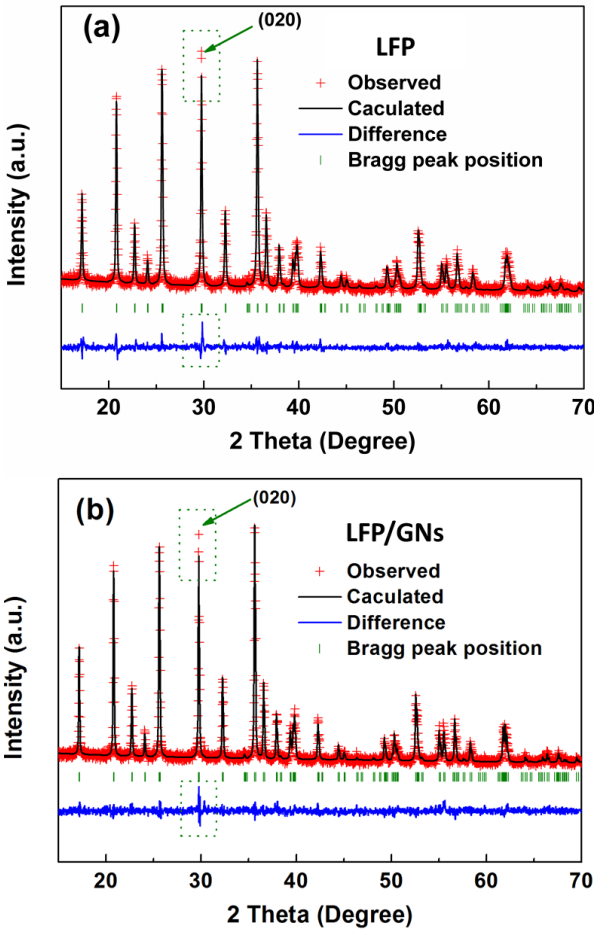

Fig. S6† XRD patterns as well as the Rietveld refinements of LFP (a) and LFP/GNs (b).

All diffraction peaks seen from both LFP and LFP/GNs can be indexed to crystalline LFP with a space group of *Pnma* (JCPDS No. 81-1173), which proved that the introduction of graphene had no effect on the structure of LFP. The sharp peaks seen indicate that the samples are well crystalline. No obvious peaks corresponding to graphene were found owing to the low graphene content and the strong (111) diffraction peak of LFP crystal, which shadowed the (002) peak at the similar 2θ.[3,4] The fit between observed and calculated patterns were good, which indicated that all elements were well located in their crystallographic sites, as shown in Table S2†. The resulting lattice parameters obtained from the Rietveld refinement of LFP were a = 10.3283 Å, b = 6.0062 Å, and c = 4.6919 Å, as to LFP/GNs, the lattice parameters were a = 10.3276 Å, b = 6.0064 Å, and c = 4.6915 Å. Both sets of the values were in good agreement of JCPDS 81-1173 (a = 10.332 Å, b = 6.01 Å, and c = 4.692 Å), indicative of the high purity. Analogously, a large mismatch of the (020) peak could also be observed and the $I_{(020)}/I_{(200)}$ ratios for LFP and LFP/GNs were 3.07 and 2.93 respectively, which were much larger than the standard value (2.08), implying the (010) facet oriented platelet morphology of the LFP crystals.[5,6]

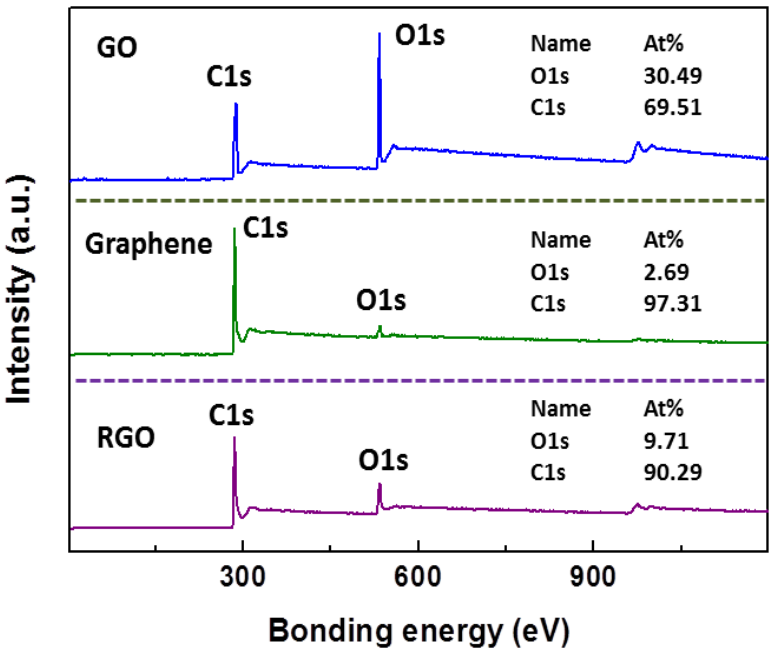

Fig. S7† Comparason of the chemical composition of GO, EG chemically reduced graphene and thermally reduced grahene oxide (RGO).

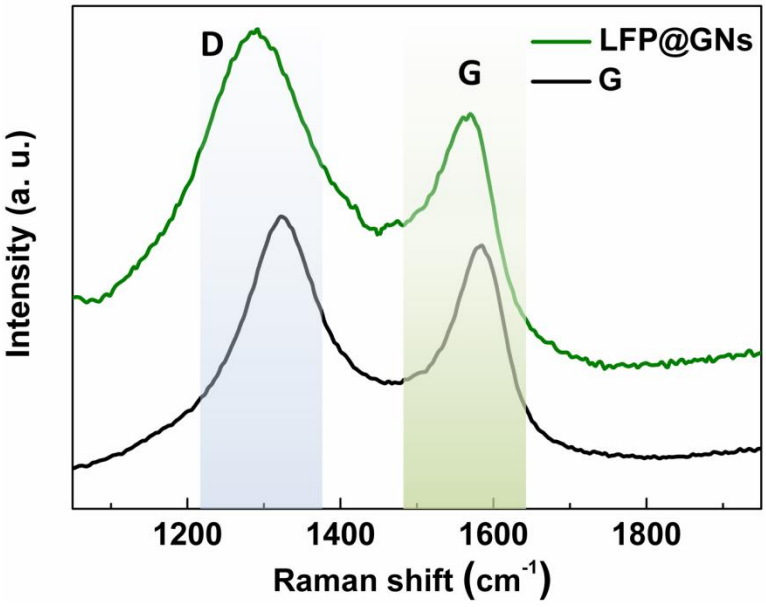

Fig. S8† Comparison of the Raman spectrum of LFP@GNs and EG reduced graphene.

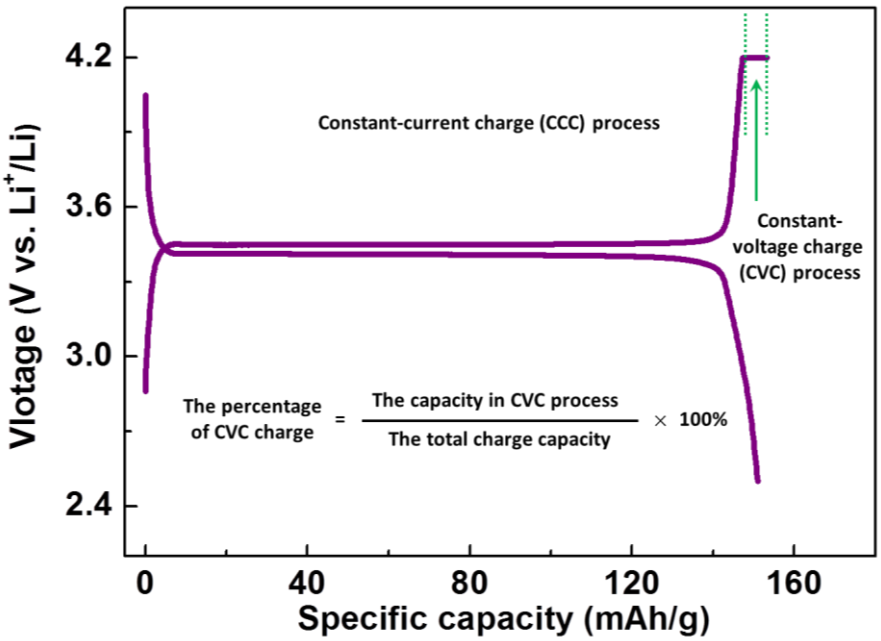

Fig. S9† The typical charge/discharge curve of LFP/GNs at 0.2C. Inset shows the calculation formula of the capacity percentage of constant-voltage charge.

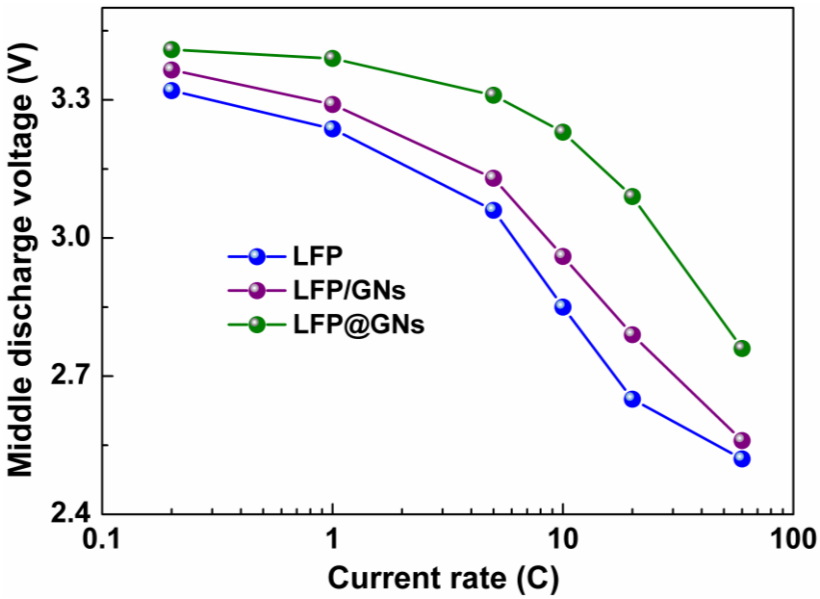

Fig. S10† The dependency of the middle discharge voltage on current rate in the range of 0.2C to 60C for LFP, LFP/GNs and LFP@GNs.

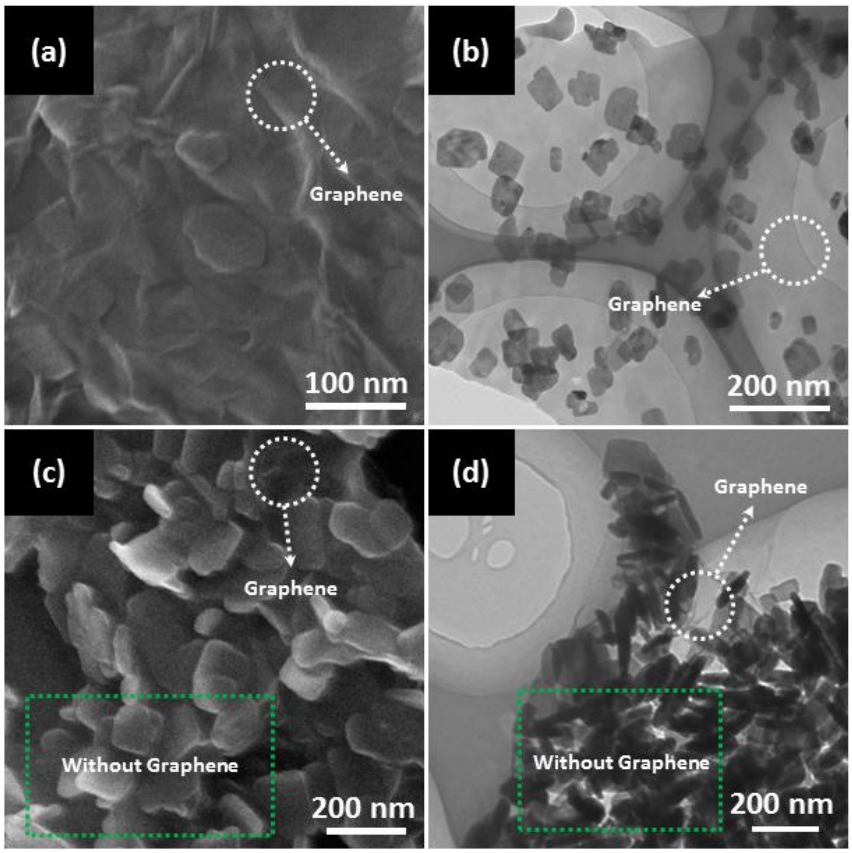

Fig. S11† SEM and TEM images of LFP@GNs (a, b) and LFP/GNs (c, d) electrodes after 1000 electrochemical cycles at 10C.

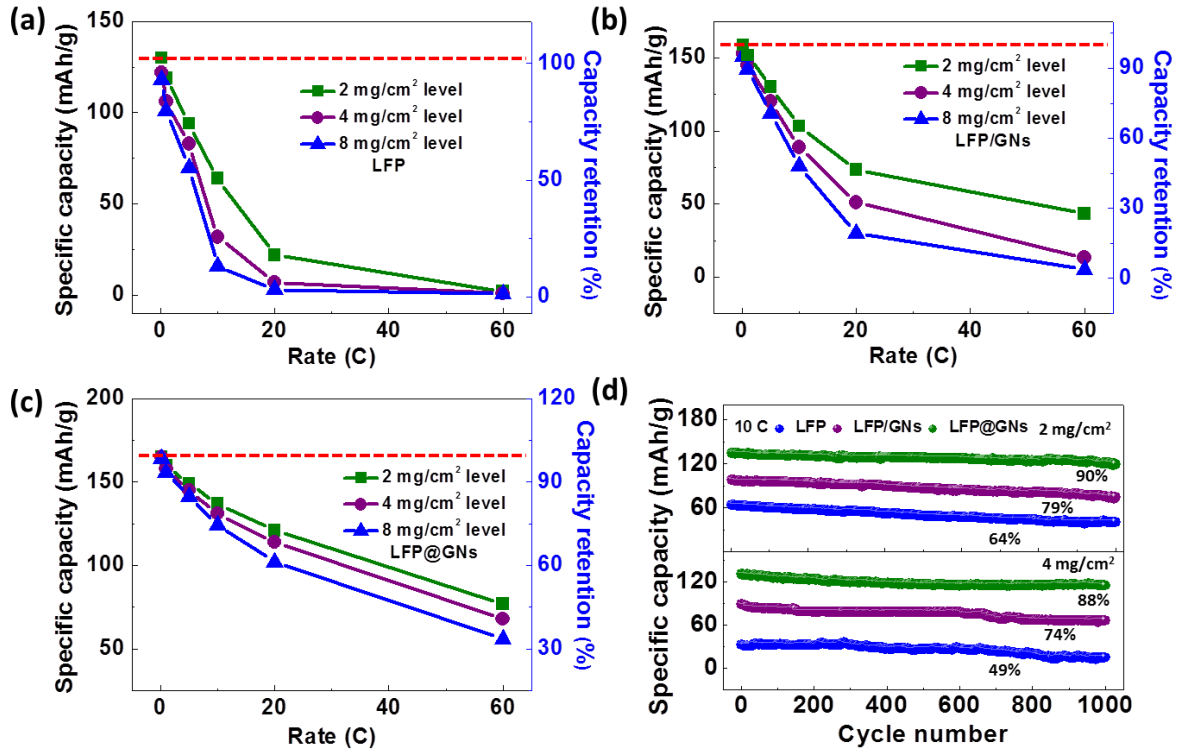

Fig. S12† Electrochemical performance of LFP, LFP/GNs and LFP@GNs electrode with different mass loading: (a-c) rate performance and (d) cycling stability at 10C.

It can be seen that the capacity and cycling stability of LFP/GNs and LFP decayed rapidly with the increase in the loading mass due to the increased polarization, especially along the direction perpendicular to the current collector. While for LFP@GNs, the capacity retention and cycling stability were still much better than LFP/GNs and LFP, suggesting the inside 3D porous conductive network effectively facilitate both Li^+ and electron transport, and thus, reducing the polarization.

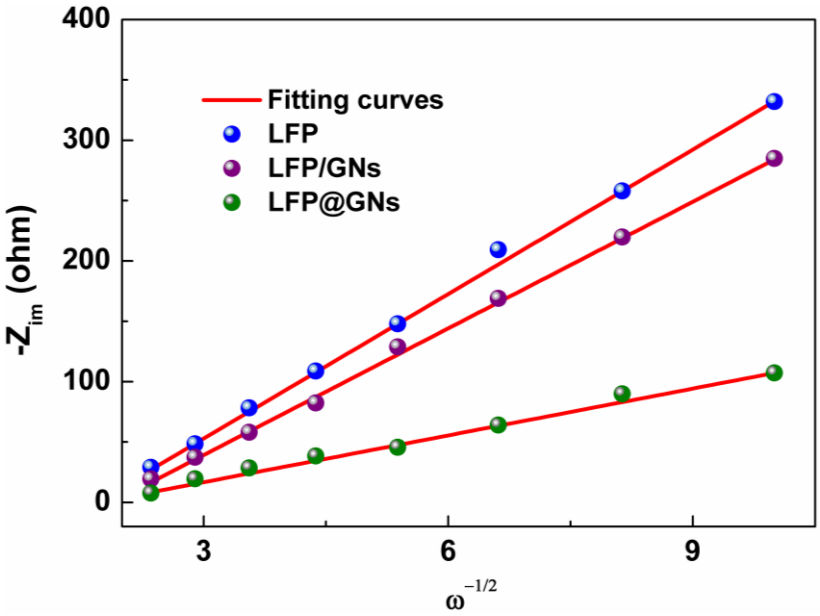

Fig. S13† Variations and fittings between $-Z_{im}$ and the reciprocal square root of the angular frequency in the low-frequency region of LFP, LFP/GNs and LFP@GNs.

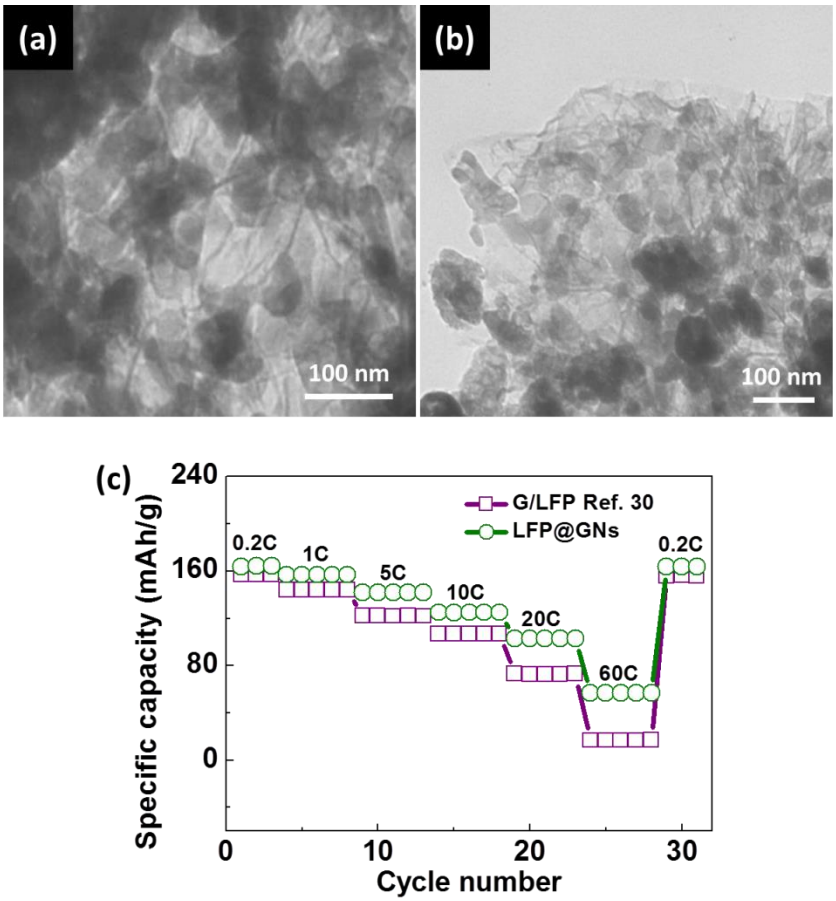

Fig. S14† (a, b) TEM images of a LFP/G composite[30] which has a similar BET surface area with LFP@GNs of this work and (c) Comaprsion of the rate performance of LFP/G[30] with LFP@GNs.

In order to further confirm the positive role of (010) facets anchored on graphene, we supplemented a comparison study of LFP@GNs with a G/LFP composite (similar BET surface area, 8 $mg \cdot cm^{-2}$ mass loading), in which the irregular LFP nanoparticles with dimension ranged from 20~60 nm anchored on graphene as we reported previously.[30] As can be seen, the rate performance of LFP@GNs was much better than G/LFP, especially at a high rate ($\geq$ 20C), and thus further demonstrate the positive role of (010) facets anchored on graphene.

Tables

Table S1† Summary of LFP/graphene composites synthesized by different methods with different LFP crystal morphology and composite structure.

Ref.	Preparation of GO	Reduction of GO	Synthesis	Structure	Specific capacity ($mAh \cdot g^{-1}$)
13	Hummers method	Thermal	Sol-gel	Graphene embedded in micron-sized porous LFP bulk	146 (0.1C)/~90 (1C)/~50 (10C)
14	Hummers method	Chemical (ascorbic acid)	Hydrothermal	Graphene mixed with LFP particle (~100-300 nm)[a]	160.3 (0.1C)/~125 (1C)/81.5 (10C)
15	Hummers method	Chemical (hydrazine hydrate)	Solvothermal	Graphene mixed with LFP particle (200-400 nm)[a]	162 (0.1C)/138 (1C)/114 (10C)
16	Modified hummers method	Chemical (tetraethyleneglycol)	Microwave-solvothermal	LFP nanorods (width: ~100 nm; length: ~ 200-600 nm) decorated on graphene[b]	164 (0.1C)/~145 (1C)/~100 (5C)
17	Modified hummers method	Chemical (hydrazine)	Solvothermal	LFP particle (30-250 nm) *in situ* grow on graphene[a]	~160 (0.1C)/72.7 (20C)/42 (40C)
18	Modified hummers method	Chemical ($FeCl_2$)	Solid-state	Graphene dispersed in LFP particles[a]	161.3 (0.2C)/141.5 (1C)/115 (10C)
19	—		Solvothermal	LFP particles dispersed in graphene substrate[a]	152 (0.01 $A \cdot g^{-1}$)/100 (5 $A \cdot g^{-1}$)
20	Vacuum-promoted low-temperature approach		Mechanical mixing	LFP particles *ex situ* mixed with graphene[a]	~150 (0.05C)
21	Modified hummers method	Thermal	Spray drying	Graphene wrapped primary LFP particles (50-100 nm) with secondary microsphere diameter of 2-5 um[a]	148 (0.1C)/86 (30C)
22	Hummers method	Chemical (ascorbic acid)	Microwave-hydrothermal	LFP particles (~150 nm) wrapped by graphene[a]	165 (0.1C)/88 (10C)
23	Modified hummers method	Thermal	Solid-state	Graphene encapsulated LFP nanoparticles (~20 nm)[a]	166.6 (0.1C)/108.6 (5C)/90.6 (10C)
24	Graphene deposited on a porous nickel substrate via a CVD method, followed by dissolution of nickel in HCl		Mechanical mixing	LFP particles (0.5-1 um) dispersed in 3D graphene conductive network[a]	158 (0.2C)/150 (1C)/ 109 (10C)
25	Modified hummers method	Thermal	Ultrasonic-assisted rheological phase method	LFP nanoparticles (< 100 nm) wrapped by graphene sheet or embedded in graphene sheets[a]	160 (0.2C)/150 (1C)/116 (20C)
26	Modified hummers method	Chemical (ethylene glycol)	Hydrothermal	LFP nanorods (30-100 nm in diameter and 80-400 nm in length) embedded in graphene matrix[b]	~160 (0.1C)/~100 (20C)/79.7 (50C)
27	Commercial graphene flakes (Graphene Supermarket, average flake thickness = 8nm, average particle size = 550 nm, and electrical conductivity ~10^5 $S \cdot m^{-1}$)		Electrospinning	Graphene homogeneously dispersed in LFP fibres (163 nm in diameter)	163 (0.05C)/132 (1C)/107 (2C)
28	Hummers method	Thermal (stacked graphene); chemical (hydrazine, unfolded graphene)	Solid-state	Stacked graphene dispersed in micro-scale LFP particles; LFP nanoparticles anchored to the unfolded graphene matrix[a]	86 (0.1C) for stacked graphene modified composite; 166.2 (0.1C)/~100 (5C)/75 (10C) for unfolded graphene modified composite
29	Modified hummers method	Chemical (tetraethyleneglycol)	Polyol method	Graphene-wrapped LFP nanorods, width: 20 nm; length: 50 nm[b]	164 (0.1C)/156.7 (1C)/121.5 (10C)
30	Modified hummers method	Thermal	Modified rheological phase method	Mesoporous LFP nanoparticles (20-60 nm) wrapped by graphene[a]	156 (0.2C)/~145 (1C)/~100 (20C)
31	Modified hummers method	Chemical (hydrazine hydrate)	Co-precipitation method	LFP nanoparticles (~20 nm) adhered to the surface of graphene[a]	160 (0.2C)/146 (1C)/109 (10C)
32	—		In situ graphitizing organic interlayer	Sandwich-like nanostructure[c]	168 (0.5C)/159 (1C)/ 117 (10C)
33	Hummers method	Thermal	Self-assembly	LFP nanoparticles (~100 nm) embedded in graphene network[a]	~145 (1C)/~136 (2C)/110 (10C)
34	Modified hummers method	Chemical ($NaBH_4$ and hydrazine hydrate)	Mechanical mixing	LFP nanoparticles assembled on graphene[a]	165 (0.5C)/151 (1C)/115 (10C)
35	Hummers method	Thermal	Self-assembly	Graphene sheets embedded in LFP macroparticles[a]	155 (0.1C)/130 (1C)/103 (10C)
36	Heat-treatment combined with ultrasonic		Mechanical mixing	LFP particle adhered to the surface of graphene[a]	139.1 (1C)/121.9 (10C)/107.8 (20C)
This work	Modified hummers method	Chemical (ethylene glycol)	Solvothermal	LFP nanoplates (80~100 nm in length, 40~60 nm in width and 10~20 nm in thickness) *in situ* grew on graphene and further formed a graphene cross-linked structure[d]	164 (0.2C)/155 (1C)/100 (20C)/56 (60C)

[a]"particle-on-sheet" mode with "point-to-point" electronic contact; [b]"nanorod-on-sheet" mode with "line-to-point" electronic contact; [c]"sandwich-like" mode and [d]"platelet-on-sheet" mode with "face-to-face" electronic contact.

Table S2† Results of structural analysis obtained from XRD Rietveld refinement of LFP, LFP/GNs and LFP@GNs.

Samples	Atoms	Site	X	Y	Z	Occupancy	Ui/Ue×100
LFP	Li	4a	0	0	0	1	0.36
(*a*=10.3283Å,	Fe	4c	0.2827	0.25	0.9762	1	0.61
b=6.0062Å,	P	4c	0.0972	0.25	0.4176	1	-0.86
c=4.6919Å;	O1	4c	0.0975	0.25	0.7406	1	-0.93
R_{wp}=6.49%;	O2	4c	0.4635	0.25	0.2053	1	1.75
R_p=5.62%; χ^2=1.26%)	O3	8d	0.1538	0.0476	0.2847	1	1.62
LFP/GNs	Li	4a	0	0	0	1	0.51
(*a*=10.3276Å,	Fe	4c	0.2863	0.25	0.9764	1	-1.13
b=6.0064Å,	P	4c	0.0961	0.25	0.4276	1	-1.85
c=4.6927Å;	O1	4c	0.0982	0.25	0.7531	1	-0.37
R_{wp}=6.92%;	O2	4c	0.4592	0.25	0.2046	1	1.02
R_p=5.93%; χ^2=1.63%)	O3	8d	0.1542	0.0463	0.2854	1	1.52
	Li	4a	0	0	0	1	0.27
	Fe	4c	0.2851	0.25	0.9773	1	1.31
LFP@GNs	P	4c	0.0957	0.25	0.4256	1	0.61
(*a*=10.3281Å,	O1	4c	0.0972	0.25	0.7514	1	-1.63
b=6.0059Å,	O2	4c	0.4586	0.25	0.2029	1	-1.87
c=4.6906Å;	O3	8d	0.1537	0.0465	0.2874	1	-0.93
R_{wp}=6.52%;	Fe	4c		—		1	—
R_p=6.03%;	P	4c		—		1	—
χ^2=1.17%)	O1	4c		—		1	—
	O2	4c		—		1	—
	O3	8d		—		1	—

Table S3† Results of the statistical calculation of the proportion for (010) facet of LFP, LFP/GNs and LFP@GNs.

Samples	*Length(ab)*/nm	*Width(bc)*/nm	*Thickness(be)*/nm	the proportion of (010) facet/%
LFP	176.26	86.13	38.45	60.44
LFP/GNs			similar to LFPNP	
LFP@GNs	96.79	53.67	14.23	70.76

Table S4† The fitting values of the resistance components in the simplified equivalent circuit.

Samples	R_Ω/Ω·cm^{-2}	R_1/Ω·cm^{-2}	R_2/Ω·cm^{-2}
LFP	6.4	23.6	245.5
LFP/GNs	4.9	11.5	138.7
LFP@GNs	2.9	6.8	21.6

References

1. Q. M. Wang, D. L. Wang and B. Wang, *Ionics*, 2013, **19**, 245.
2. J. Ha, S. K. Park, S. H. Yu, A. H. Jin, B. Jang, S. Bong, I. Kim, Y. E. Sung and Y. Piao, *Nanoscale*, 2013, **5**, 8647.
3. B. Wang, D. L. Wang, Q. M. Wang, T. F. Liu, C. F. Guo and X. S. Zhao, *J. Mater. Chem. A*, 2013, **1**, 135.
4. F. Zhou, F Wang, Y. M. Zhu and Z. P. Liu, *J. Mater. Chem.*, 2011, **21**, 3353.
5. K. Dokko, S. Koizumi, H. Nakano and K. Kanamura, *J. Mater. Chem.*, 2007, **17**, 4803.
6. L. Wang, X. M. He, W. T. Sun, J. L.Wang, Y. D. Li and S. S. Fan, *Nano Lett.*, 2012, **12**, 5632.